Influence of curing temperature on the evolution of magnesium oxychloride cement

Vincenzo M. Sglavo · Francesca De Genua ·
Alexia Conci · Riccardo Ceccato · Roberto Cavallini

Abstract Hardening behaviour and strength of oxychloride cement strongly depend on the formation of Phase 3 and Phase 5 from MgO and magnesium chloride water solution, and the initial composition can be chosen accordingly within the corresponding phase diagram. A certain number of reactions occur before the final formation of P5 or P3 crystals, and several parameters influence the transformations kinetic, such as MgO reactivity and temperature. Several articles deal with the first aspect, while no indications can be found with regard to the curing temperature's effect on the formation of noble phases. In this article the evolution of magnesium oxychloride cement pastes is analysed at various curing temperatures between 5 and 40 °C. The study is carried out to simulate typical industrial processing conditions and indicate optimal conditions for the production of high chemical and mechanical resistance oxychloride cement. It is shown that at low temperature, Phase 3 is produced in place of Phase 5, and a certain amount of MgO remains non-reacted. The corresponding cement is characterised by lower mechanical strength and higher water solubility.

Introduction

Magnesium oxychloride cement (MOC), also known as Sorel cement, is a type of non-hydraulic cement that was discovered by a Frenchman, Sorel [1]. It is obtained by

V. M. Sglavo (✉) · F. De Genua · A. Conci · R. Ceccato
DIMTI, University of Trento, Via Mesiano 77,
38123 Trento, Italy
e-mail: vincenzo.sglavo@unitn.it

R. Cavallini
Deroma Spa, Via Pasubio 17, 36034 Malo, VI, Italy

mixing magnesium oxide (MgO) powder with a concentrated solution of magnesium chloride ($MgCl_2$).

Magnesium oxychloride cement has many interesting properties as compared to ordinary Portland cement. First of all, the specific density is significantly lower. It possesses high compressive and flexural strengths, elevated fire resistance, low thermal conductivity, good resistance to abrasion and is unaffected by oil, grease and paints. Mechanical strength is developed in a relatively limited time and, in addition, MOC is suitable for use with large quantities of different aggregates, including gravel, sand, marble flour, wood particles and expanded clays. The lower alkalinity of MOC (pH of 10–11) compared with the higher one of ordinary cement (pH of 12–13) makes it suitable for use with glass fibres. It has been used primarily as flooring material by virtue of its elastic and acoustic properties, resistance to accumulation of static charge and its attractive marble- or ivory-like appearance. Some other major applications of MOC include fire protection systems and grinding wheels, wall insulation panels, stuccos with revealed aggregates, decorative elements and vases [2–7]. MOC has also been successfully used as absorbent substrate for removing chromium, thorium or uranium from wastewater [8, 9].

However, some difficulty has been encountered in the use of oxychloride cements especially for exterior applications or in employments, where contact with water is possible; as a matter of fact, problems of dimensional instability, lack of resistance to weathering and release of corrosive solutions have been severe in some cases [4, 10].

It is well known that two hydrate phases, $5\,Mg(OH)_2 \cdot MgCl_2 \cdot 8H_2O$ (phase 5 or P5) and $3\,Mg(OH)_2 \cdot MgCl_2 \cdot 8H_2O$ (phase 3 or P3) are the fundamental reaction products responsible for hardening and strength development of MOC. In particular, the formation of needle-like phase 5

crystals in the hydrated cement is desirable, as it is widely reported that such crystals provide the best mechanical properties [13].

According to Li and Chau [13], with MgO:MgCl$_2$ molar ratios between 5 and 6 and stoichiometric amount of water [required for complete transformation of MgO into phase 5 and the excess into Mg(OH)$_2$], or a slight water excess (necessary for workability of pastes), the reaction products are phase 5 and some Mg(OH)$_2$ [13]. Under these conditions, at room temperature, phase 5 remains stable, if not reacted with water or carbon dioxide [12, 14, 15]. Phase 5 soon appears (about 2 h after the paste is mixed) in the form of needle-like crystals which interlock in a rapid growth. When growth is inhibited by lack of space, the crystals intergrow into a denser structure. Therefore, it is claimed that the strength depends on the formation of phase 5, which has good space-filling properties, and forms a dense microstructure of minimum porosity [11, 12].

For normal industrial or laboratory practice, it is believed that the chemical reactions in the system MgO–MgCl$_2$–H$_2$O are usually not complete, and many unreacted MgO particles are expected to remain in the final product [13]. While unreacted MgO fragments can be treated as filler, chloride ions in excess, however, are troublesome as they can cause corrosion problems in the case of involvement of reinforcing steels. Moreover, higher water content is usually required as a plasticiser for the required workability of the paste. Therefore, magnesium oxide and water in excess to theoretical loads are suggested for being used in the production of phase 5 containing MOC cement while keeping the free chloride ions to the minimum. In a recent article, the optimal ranges of the MgO/MgCl$_2$ and H$_2$O/MgCl$_2$ molar ratios within the ternary system of MOC cement are identified as 11–17 and 12–18, respectively. The choice of the H$_2$O/MgCl$_2$ molar ratio is shown to be, however, largely depending on the molar ratio of MgO/MgCl$_2$ as excess water is required for preferred workability. The most critical molar ratio to be selected in the design process of MOC cement is therefore the latter one, the optimal value being reported as equal to 13 [13]. With regard to the phase diagram of the ternary system MgO–MgCl$_2$–H$_2$O at room temperature (25 ± 3 °C) [9, 13], the optimal composition for MOC cement should lie more or less in the middle of the compatibility triangle MgO–P3–P5 as shown in Fig. 1 [13].

It has also been shown in previous studies that the correct or theoretical proportions of the starting materials alone are not sufficient to ensure the formation of phase 5 crystals, since other factors such as the reactivity of MgO can have a strong influence [12]. If one considers the complicated network of reactions that occur before final formation of P5 or P3 crystals, then several parameters influencing the transformations kinetic such as MgO reactivity and temperature, must be considered [16, 17]. A number of important articles
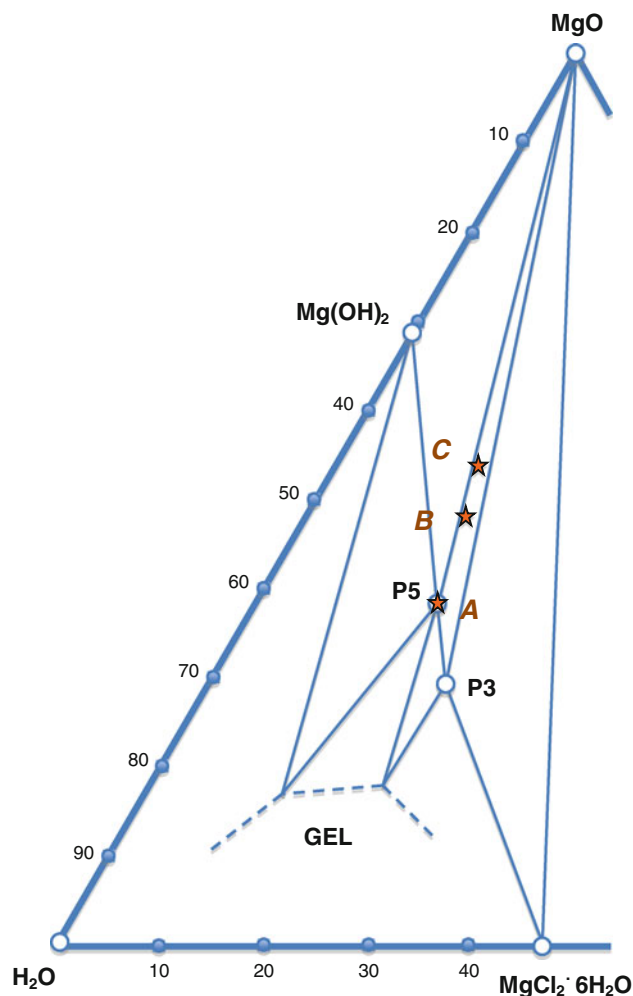

Fig. 1 Isothermal section in the range of 20–26 °C of the system MgO–MgCl$_2$–H$_2$O [12, 13]; the compositions of the cements (*A*, *B* and *C*) studied here are shown by *stars*

report in detail the effect of MgO microstructure associated to various calcination temperatures of the starting carbonate or hydroxide, on its reactivity with MgCl$_2$ solutions and on final products [10, 12, 16]. Nevertheless, no detailed information can be found with regard to the effect of temperature on reactivity and resultant phases. In our opinion, due to the relatively high velocity of the reactions occurring in the formation of MOCs, temperature should assume an important role in controlling the composition and, therefore, the quality of the final product. In industrial practice, the control of processing temperature is not unquestionable as some activities are performed in open air spaces where environmental conditions can vary drastically between night and day and which also influenced by weather and seasonal conditions. On this basis, the same recipe for MOC production applied in industrial plants located in different locations or in different seasons could lead to quite different results, thus negatively affecting the quality and reproducibility of the products.

In this study, the evolution of oxychloride phases as a function of initial composition, curing temperature and time is analysed. MOC pastes, prepared on the basis of previous works guidelines [13] to obtain P3 and P5 phases, are considered and curing temperatures between 5 and 40 °C are used in order to simulate typical industrial processing conditions and indicate optimal conditions for the production of high chemical and mechanical resistance oxychloride cement.

Experimental procedure

Commercially available magnesium oxide (MgO-Periclase) (Kirsch Pharma GmbH, Salzgitter, Germany) and hexahydrate magnesium chloride ($MgCl_2 \cdot 6H_2O$) (Chemische Fabrik Lehrte GmbH, Lehrte, Germany) were used for the preparation of MOC paste. MgO consists of calcined magnesite powder with purity in excess of 98.8%. Magnesium chloride powder is also substantially pure (>99.5%). Deionized water was also used for the production of cement.

Magnesium oxychloride cement with three distinct compositions as indicated in Fig. 1 was prepared. According to previous studies [13], in order to produce high mechanical resistance MOC, $MgO:MgCl_2$ molar ratio was varied between 5 and 9, maintaining the composition within the compatibility triangle MgO–P3–P5 (Fig. 1) constant. The composition of the cement paste considered here is reported in Table 1; $MgO:MgCl_2$ and $H_2O:MgCl_2$ molar ratios are also shown for comparison.

Initially, magnesium chloride was completely dissolved in deionized water before mixing with MgO powder.

MOC was prepared and cured at constant temperatures ranging from 5 to 40 °C. Raw materials were stored at the preferred temperature for at least 12 h before use. Magnesium chloride water solution was prepared at first, with MgO powder being added just after the solubilisation of $MgCl_2 \cdot 6H_2O$. The paste was stirred manually for about 5 min and then cast into silicone moulds, which were sealed with polyethylene film, allowing the cement to cure for the specified amount of time.

The consistency of the cement paste was constantly monitored to analyse the hardening process as a function of time and temperature. To do this, a small pin with flat-head (1-mm diameter) was pressed at regular time intervals on the surface of the sample by the application of a limited load (around 0.1 N) and hardening onset was determined when the loaded pin could not penetrate the specimen, such situation guaranteeing the possibility of extracting the cement specimen from the mould without failures or damage.

At specified time intervals, portions of sample were collected, reduced to powder and subjected to qualitative analysis by X-ray diffractometry (XRD) using CuKα radiation at 40 kV and 30 mA (Geiger Flex Dmax III, Rigaku Inc., Tokyo, Japan); a graphite monochromator was inserted in the diffracted beam. Powder samples were scanned in the 10°–80° (2θ) interval with 0.05° sampling interval and 5 s counting time.

Jade 8 software (MDI Materials Data Inc., Livermore CA, USA) was employed to perform qualitative analysis. Quantitative analysis of the phases detected in the samples as a function of curing time was carried out using MAUD software [18], a modified Rietveld method for the evaluation of the content of amorphous and crystalline phases in ceramic samples [19].

Cements of different composition cured at 10 and 28 °C for 1 week were subjected to mechanical tests. In this case, silicone moulds that allow the production of discs (30-mm diameter, 4-mm thickness) were used. The piston-on-three-balls configuration [20] was used by an universal mechanical testing machine (mod. 810, MTS Systems, Minneapolis, MN, USA). Care was taken to place the surface previously in contact with the mould in tension. The discs were supported on three steel balls (3.2-mm diameter) lying on a circle of 25 mm diameter, 120° apart. The load was applied at the centre of the disk by a hardened steel cylinder (1.5-mm diameter).

The broken samples were used for microstructural investigations by scanning electron microscopy (SEM) (JSM-5500, Jeol Inc., Tokyo, Japan).

Solubility tests were also carried out on cements cured at 10 and 28 °C for 1 week. In this case, silicone moulds allowing the production of cylinders (15-mm height, 30-mm diameter) were used. The samples were initially placed in deionized water for 4 h at 25 °C; the solution was then analysed by plasma emission spectrometry (ICP-OES) (Spectro Ciros, SPECTRO Analytical Instruments GmbH, Kleve, Germany) to measure the concentration of Mg^{2+} and Cl^- ions.

Results and discussion

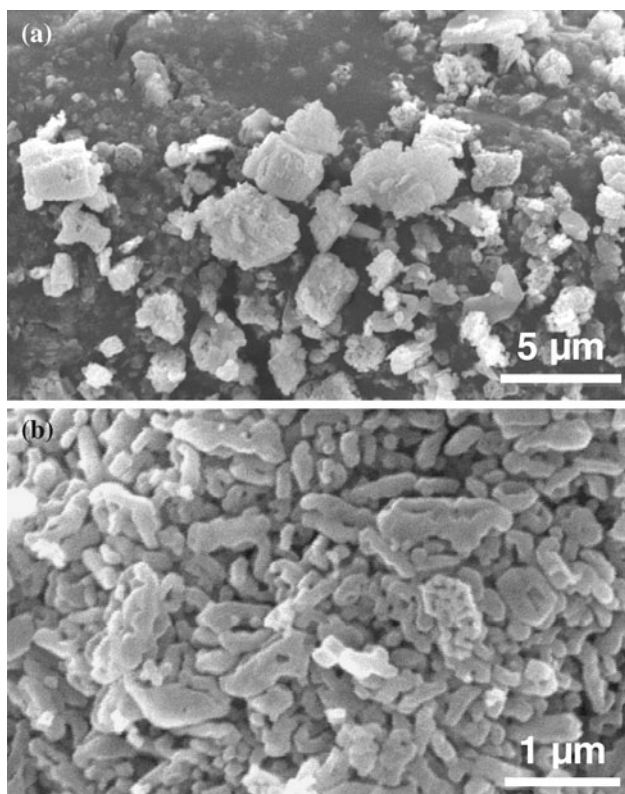SEM observations (Fig. 2) of starting powders revealed an aggregate morphology for both MgO and magnesium

Table 1 Composition (wt%) of the cements studied in this study

	A	B	C
MgO	38.0	47.5	53.8
$MgCl_2 \cdot 6H_2O$	38.3	34.3	30.2
Deionized water	23.7	18.2	16.0
$MgO:MgCl_2$ molar ratio	5	7	9
$H_2O:MgCl_2$ molar ratio	13	12	12

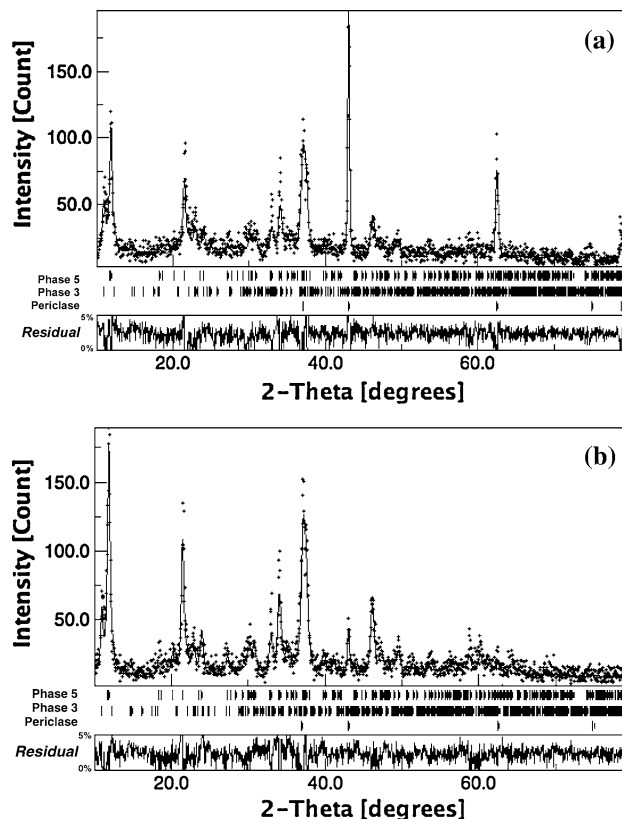Fig. 2 SEM micrograph of MgCl$_2$ (a) and MgO (b) powders used in this study

Fig. 3 Fitting plots for the quantitative XRD analysis carried out on cements with composition A, cured at 17 °C for duration of **a** 29 h and **b** 198 h. The single points and the *solid line* correspond to the experimental and calculated XRD pattern, respectively. The residual of the least-square fitting procedure is shown underneath each diagram

chloride, the former showing an average size of the constituting grains around 0.2–1 μm.

The analysis of the consistency of the cement paste upon ageing in sealed moulds revealed an important effect of curing temperature. Just after the addition of MgO powder to chloride solution, the mixture varied from liquid state in sample A to very viscous state in composition C. The consistency evolved very slowly at the temperature of 5 °C: the specimens could be extracted from the mould with great care only after 24–28 h though being still very brittle and soaked in water, especially for compositions A and B. The behaviour was drastically different at 17 °C, where samples revealed solid texture after 24 h, with no sign of residual macroscopic non-reacted water. The same appearance was evident for all compositions after only 4–5 h if cements were cured at temperatures in excess to 25 °C.

Qualitative analysis of the XRD spectra pointed to the presence of only three phases: MgO-Periclase (PDF n. 45-946); MO—Phase 3, corresponding to the mineral phase Mg$_2$(OH)$_3$Cl·4H$_2$O (PDF n. 7-412) and MO—Phase 5, corresponding to the mineral phase Mg$_3$(OH)$_5$Cl·4H$_2$O (PDF n. 7-420) [21]. No other phases were detected in any of the analysed samples.

On this basis, quantitative analyses were performed using the Rietveld-modified evaluation method as previously

defined. Calculated patterns of the three detected phases (Fig. 3) were determined from their crystallographic data and the corresponding ICSD codes: 31051 for Periclase, 24668 for Phase 3 and 2103035 for Phase 5, respectively [22]. The least-square fitting procedure was iterated until the residual was lower than 5% for each 2θ value (Fig. 3). As an example of the used procedure, two fitting plots are reported in Fig. 3, corresponding to the composition A cured at 17°C for durations of 29 and 198 h. The results show an increase of Phase 5 from 49 to 76%, while Periclase and Phase 3 decrease from 22 to about 3% and from 29 to 20%, respectively.

The overall evolution of mineral phases as a function of curing time for cements produced and stored at different temperatures is shown in Fig. 4. For some composition/temperature/curing time conditions the analysis was repeated on different samples, and the results indicate that an uncertainty of 5% at the most can be considered in the analyses of reported data, this being the combination of small temperature differences (1–2 °C) upon mixing and curing and the error associated with the modified Rietveld
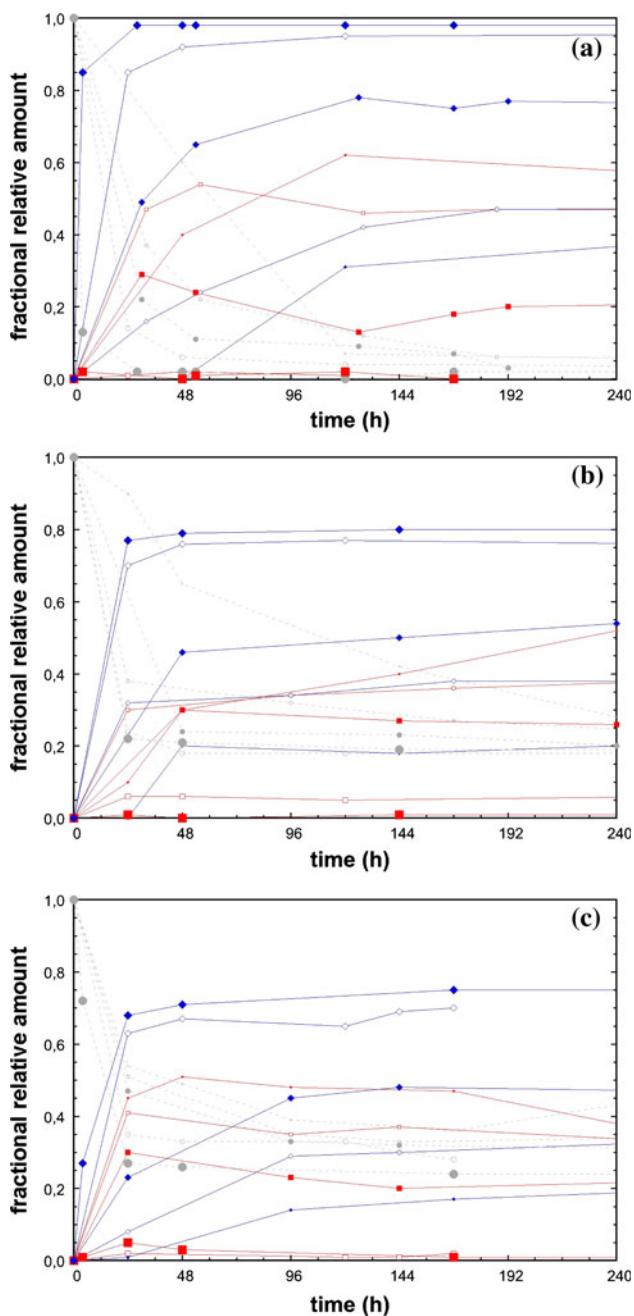
Fig. 4 Evolution of mineral phases (MgO—*circles*, P3—*squares* and P5—*diamonds*) with curing time in oxychloride cement A (**a**), B (**b**) and C (**c**). The size of the symbols increases as curing temperature changes with the sequence 5, 10, 17, 28 and 40 °C

XRD quantitative analysis. Most tests were prolonged for very long duration, and composition did not change within the defined error neither for curing times in excess of 1 month at the fixed initial temperature. It is worth pointing out that the results reported in Fig. 4 correspond to samples stored in a close environment at fixed temperature, without any chemicals' exchange with external atmosphere. Time equal to $\approx$ 10 days is definitely much longer than typical

duration for an industrial process, where MOC components must be produced and be kept in an insulated environment for about a few hours. Therefore, the results presented here are of fundamental importance to evaluate evolution of mineralogical phases in the material during a typical industrial production.

In order to have an easy reading of Fig. 4, it should be specified that phase 3 was almost not detected in cements A and B cured at temperatures equal to or higher than 28 °C, and in cement C cured at 40 °C.

Some important observations can be drawn from the analysis of the reported diagrams. First of all, the evolution towards Phase 3 or Phase 5 is clearly faster as the curing temperature increases. For example, at 40 °C, phase 5 is substantially completely formed in sample A after 48 h; in the other samples (B and C), at the same temperature, an equilibrium condition among phases is reached in about 24–48 h. Conversely, as temperature decreases, reactivity of the involved chemical species appears slower and at 5 °C, durations in excess of 100 h are necessary to reach a stable condition.

Profound differences can also be observed when compositions A, B and C are compared at similar curing temperatures. In sample A, there is a strong tendency for the production of phase 5 from MgO at very high temperatures; conversely, at 10 and 5 °C, the final product is a mixture of MgO and phase 3. In sample B, and particularly, in sample C, a discrete amount of Periclase remains nonreacted regardless of the curing temperature, with phase 3 and phase 5 being formed at low and high temperatures, respectively.

It is important to underline that no other phases other than MgO, P3 and P5 were detected in the analysed materials at the considered temperatures even after very long curing times, thus indicating a strong stability of the system as that achieved after some days of ageing.
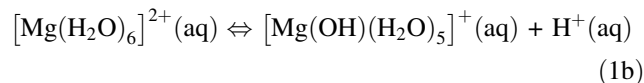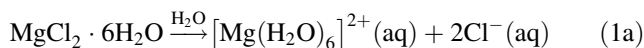
It is interesting to examine the results in Fig. 4 on the basis of the phase diagram reported in Fig. 1. Theoretically, composition A should evolve towards the unique phase 5 in the range of 20–26 °C while a residual (about 20%) MgO is experimentally observed. Only at 40 °C phase 5 is substantially observed as the unique phase in sample A. On the other hand, composition C should evolve in the range of 20–26 °C in a mixture of MgO and phase 5 (in a weight ratio of around 3:1); anomalously, the experimental data from Fig. 4 show a larger quantity of residual Periclase than that of phase 5. In some way, a certain difficulty in the formation of P3 or P5 from MgO seems to prevail, though thermodynamically predicted, considering the very fine grain size of the starting Periclase powder. Similar results have been found in previous studies, especially when relatively coarse MgO powder was used for the preparation of MOC paste [10, 11, 13]. Only when nanometric Periclase powder had

been employed, reaction products correspond to those predicted by the phase diagram [12, 16]. The results obtained from Fig. 3 can therefore be associated to kinetic effects; indeed, both P3 and P5 possess densities which are significantly lower than Periclase (1.86 for Phase 3, 1.89 for Phase 5 and 3.59 for MgO) [5]. In addition, Phase 3 and Phase 5 grow as interlocked needle-like crystals [4, 11], thus trying to occupy a large amount of volume as shown in SEM micrographs of Fig. 5. Such structure is well developed in porous regions or within bubbles, while shorter and thicker crystal appears in denser areas. Therefore, one can conclude that the use of even micrometric MgO powder does not allow the full development of needle-like structure of P3 and P5 due to the constraints caused by the surrounding material, and prevents the total consumption of Periclase phase.
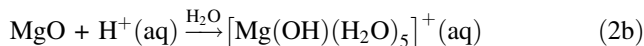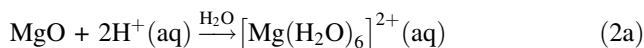
SEM micrographs were taken on cements cured for 7 days at 10 and 28 °C, and pictures taken in correspondence to bubbles and dense matrix are reported in Fig. 5, thus allowing to analyse differences in microstructure in regions, where phase evolution can occur freely (on bubbles inner surface) or is constrained by the bulk material. The analysis of micrographs reported in Fig. 5 leads to additional considerations regarding the formation of oxychlorides in MOC pastes. For example, the comparison of microstructure corresponding to compositions A and C cured at 28 °C (Figs. 5c, d, k, l) suggests a significantly longer length for P5 crystals in the former sample (5–10 μm compared to 2–5 μm on bubble surface and 1–2 μm compared to 0.2–0.5 μm in the bulk), this being related to the larger amount of such phase formed after 7 days ageing time as shown in Fig. 4 (85% compared to 45%). Another important issue is with regard to P3 crystals: it is clear from the comparison of the structure of composition A cured at 28°C consisting of P5: 85% and MgO: 15% (Fig. 4a) with that of B cured at 10 °C consisting of P3: 40% and MgO: 60% (Fig. 3b), that Phase 3 needle-like crystals (visible in Fig. 5e) are slightly longer than P5 crystals taking into account that the relative amount of oxychlorides is much smaller (40%) in the second sample with respect to the former one (85%).

Another important aspect that can be interpreted from Fig. 4 concerns the formation of Phase 3 at low temperature in place of Phase 5, as expected instead of from the phase diagram (Fig. 1). One can in fact observe that even in cements with composition A, a consistent amount of Phase 3 is formed at 5 and 10 °C though only P5 should appear. In order to explain the above observed behaviour, the kinetics of the formation mechanisms of the hydrate phases in MOC as analysed in detail in previous study [16] can be reconsidered. The genesis process of Phases 3 and 5 can be divided into four fundamental steps [17]:
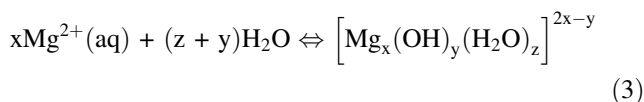
(i) dissociation of $MgCl_2$ crystals in water and consequent formation of H^+ and mononuclear complexes:
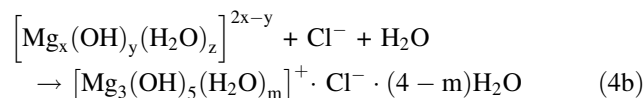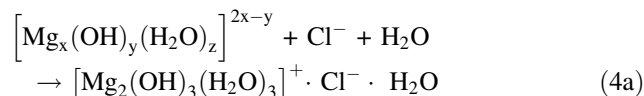
$$MgCl_2 \cdot 6H_2O \xrightarrow{H_2O} \left[Mg(H_2O)_6\right]^{2+}(aq) + 2Cl^-(aq) \quad (1a)$$

$$\left[Mg(H_2O)_6\right]^{2+}(aq) \Leftrightarrow \left[Mg(OH)(H_2O)_5\right]^+(aq) + H^+(aq) \quad (1b)$$

(ii) dissolution of MgO powder with formation of additional mononuclear complexes and increase of pH (neutralisation of MgO by H^+ ions):

$$MgO + 2H^+(aq) \xrightarrow{H_2O} \left[Mg(H_2O)_6\right]^{2+}(aq) \quad (2a)$$

$$MgO + H^+(aq) \xrightarrow{H_2O} \left[Mg(OH)(H_2O)_5\right]^+(aq) \quad (2b)$$

(iii) hydrolysis-bridging reaction of mononuclear complexes and formation of amorphous gel phases through polynuclear complexes:

$$xMg^{2+}(aq) + (z + y)H_2O \Leftrightarrow \left[Mg_x(OH)_y(H_2O)_z\right]^{2x-y} \quad (3)$$

(iv) conversion of amorphous gel phases into crystalline hydrate structures:

$$\left[Mg_x(OH)_y(H_2O)_z\right]^{2x-y} + Cl^- + H_2O$$
$$\rightarrow \left[Mg_2(OH)_3(H_2O)_3\right]^+ \cdot Cl^- \cdot H_2O \quad (4a)$$

$$\left[Mg_x(OH)_y(H_2O)_z\right]^{2x-y} + Cl^- + H_2O$$
$$\rightarrow \left[Mg_3(OH)_5(H_2O)_m\right]^+ \cdot Cl^- \cdot (4-m)H_2O \quad (4b)$$

It is clear that the reactions described by Eqs. 4a and 4b correspond to the formations of Phase 3 and Phase 5, respectively.

On the basis of the observations and results discussed previously, one can assume that temperature somehow influences the chemical reactions reported above. In particular it is not difficult to accept that the neutralisation reactions (Eqs 2a, 2b) and mainly the formation of amorphous gel through polynuclear complexes, (Eq. 3) are sensibly slowed down at low temperatures. Consequently, MgO dissolution is not complete and amorphous gel/crystalline phases are formed more slowly. Therefore, the stoichiometric ratio of the really active chemical species does not correspond any longer to the theoretical compositions defined in Table 1 and points A, B and C in the state diagram of Fig. 1 are shifted downward; for example, the actual composition corresponding to cement A will lie in the P3-P5-GEL triangle, ever closer to point P3, as the non-dissolved MgO quantity increases. On the other hand, more reaction steps are needed to form Phase 5 with respect to Phase 3 (see Eqs. 4a, 4b) and, therefore, Phase 3 formation occurs more rapidly. For these reasons, at low temperatures
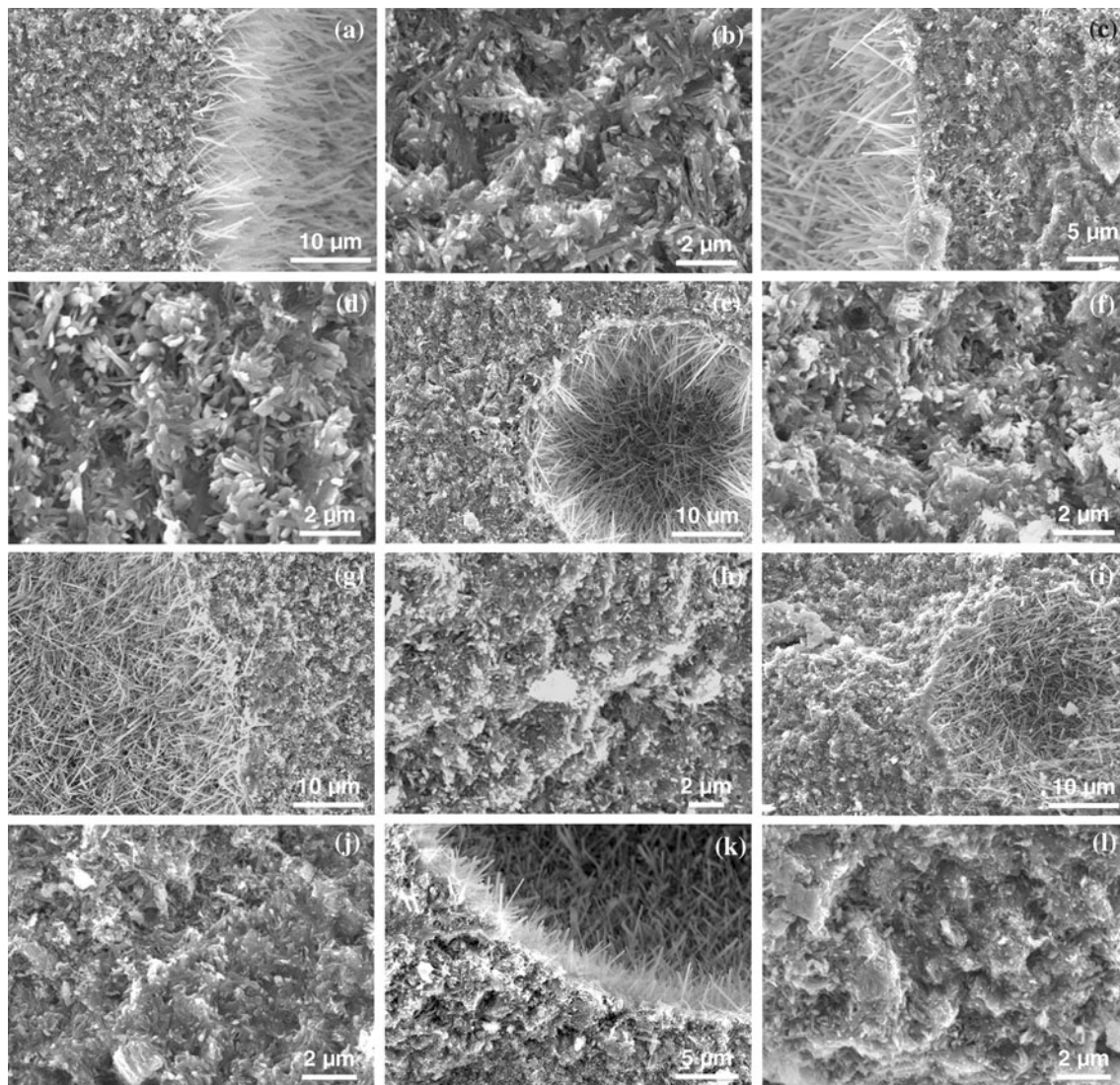
Fig. 5 Microstructure of cements after 7 days curing. Composition A stored at 10 ± 2 °C (**a, b**) and 28 ± 2 °C (**c, d**); composition B stored at 10 ± 2 °C (**e, f**) and 28 ± 2 °C (**g, h**); composition C stored at 10 ± 2 °C (**i–j**) and 28 ± 2 °C (**k, l**)

(especially at 5 and 10 °C), a certain amount of MgO remains non-dissolved, and only Phase 3 can be detected.

The macroscopic and technological importances of the evolution in MOC pastes was evaluated by mechanical and chemical resistance tests.

Figure 6 shows the flexural strength of cements cured at 10 and 28 °C. In spite of the quite large scatter of the experimental data, one can appreciate that strength is always slightly greater for the samples cured at 28 °C. This can be related to the relative amounts of 'noble' phases (P3 and P5) present in the cement after 1 week curing at the fixed temperature, which is always greater at 28 °C than at 10 °C. The strength appears also to increase slightly from composition A to C; this effect corresponds partially with previous results [13], but cannot be directly related to the amount of phase 3 or 5 as in the case of cements with

composition C in which a larger quantity of MgO is always present. The observed behaviour can be probably related to the consistency of the initial paste; for cement C, it resembles a very viscous blend, while it corresponds to a quite fluid suspension for cement A; this could account for a more interconnected structure in the former. Another reason can be found when the microstructure of cement A is compared with that of B (Fig. 5). The length/diameter ratio of needle-like phase 5 crystals occurring on pores surface appears considerably larger in composition A than in C; therefore, the development of Phase 5 in the paste of composition A could be responsible for stresses that tend to weaken the structure formed by the initial MgO particles.

The results of the dissolution tests in water are reported in Fig. 7. The experimental data are expressed as a concentration over the volume of the initial sample. The dissolution
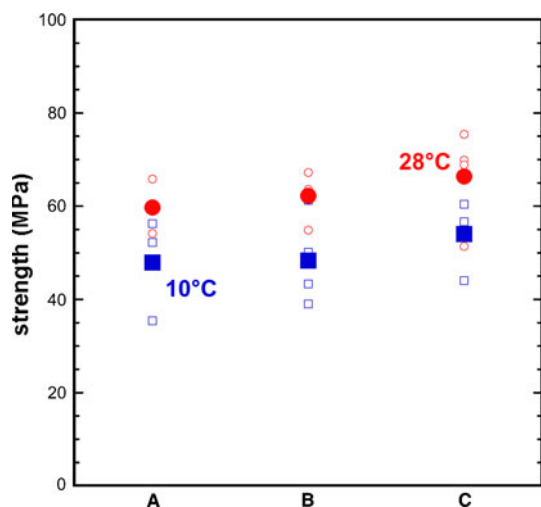
Fig. 6 Flexural strength for MOC cured at 10 °C (*squares*) and 28 °C (*circles*) for 7 days. *Large solid* symbols correspond to the average value calculated from single measurements (*small empty symbols*)
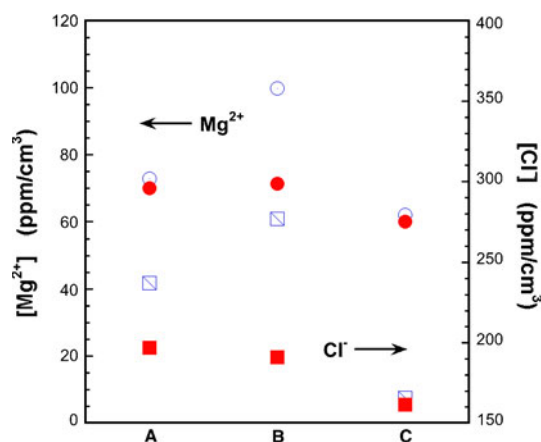

Fig. 7 Dissolution of Mg^{2+} (*circles*) and Cl^- (*squares*) from MOC cured at 10 °C (*empty symbols*) and 28 °C (*solid symbols*) for 7 days and kept in deionized water for 4 h at 25 °C

of Cl^- and Mg^{2+} ions appears more evident in the samples A and B cured at 10 °C; this can be associated with the different solubilities of Phases 3 and 5, the former being, therefore, weaker if exposed to water environment. One can easily observe the very different concentrations of Cl^- and Mg^{2+} ions in sample B cured at 10 and 28 °C, where Phase 3 and Phase 5 appear only at the two respective temperatures. As a matter of fact, no differences are shown in composition C where almost the same amount of Phase 3 and 5 is present at the two ageing temperatures.

Conclusions

The analysis of the evolution of magnesium oxychloride cement pastes at temperatures between 5 and 40 °C

highlights the influence of curing temperature on the formation of noble phases, i.e. P3 and P5. Contrary to the typical phase diagram, at low temperature Phase 3 is produced in place of Phase 5 and a certain amount of MgO remains non-reacted. This can be correlated to the complicated network of reactions responsible for the formation of Phases 3 and 5, the incomplete MgO dissolution and the slow formation of amorphous gel/crystalline phases representing the crucial steps. This effect has significant macroscopic and technological importance since the cement produced at limited temperature is characterized by lower mechanical strength and higher water solubility.

References

1. Sorel S (1867) C R Acad Sci France 65:102
2. P de Henau, M Dupas (1976) In Proceedings of the second international symposium on the deterioration of building stone, Athens, p 319
3. Skoulikidis Th, Papakonstantinou E, Galanos A, Doganis Y (1994) Study for the restoration of the Parthenon, vol 3. Ministry of Culture, Committee for the Preservation of the Acropolis Monuments, Athens
4. Maravelaki-Kalaitzaki P, Moraitou G (1999) Cem Concr Res 29:1929
5. Xia S, Xing P, Gao S (1991) Thermochim Acta 183:349
6. de Castellar MD, Lorente JC, Traveria A, Tura JM (1996) Cem Concr Res 26(8):1199
7. Plekhanova TA, Keriene J, Gailius A, Yakovlev GI (2007) Constr Build Mater 21:1833
8. Hassan SSM, Awwad NS, Aboterika AHA (2006) J Radioanal Nucl Chem 269(1):135
9. Awwad NS, Daifullah AAM (2005) J Radioanal Nucl Chem 264(3):623
10. Sorrell CA, Armstrong CR (1976) J Am Ceram Soc 59(1–2):51
11. Matkovic B, Young IF (1973) Phys Sci 246:79
12. Matkovic B, Popovic S, Rogic V, Zunic T, Young JF (1977) J Am Ceram Soc 60(11–12):504
13. Li Z, Chau CK (2007) Cem Concr Res 37:866
14. Urwongse L, Sorrell CA (1980) J Am Ceram Soc 63(9–10):501
15. Cole WF, Demediuk T (1955) Aust J Chem 8(2):234
16. Bilinski H, Matkovic B, Mazuranic C, Zunic TB (1984) J Am Ceram Soc 67(4):266
17. Dehua D, Chuanmei Z (1999) Cem Concr Res 29:1365
18. Lutterotti L, Ceccato R, Dal Maschio R, Pagani E (1998) Mater Sci Forum 278–281:87
19. Lutterotti L, Bortolotti M, Ischia G, Lonardelli I, Wenk H-R (2007) Z Kristallogr Suppl 26:125
20. Shetty DK, Rosenfield AR, McGuire P, Bansal GK, Duckworth WH (1980) Ceram Bull 59(12):1193
21. JCPDS – Joint Committee on Powder Diffraction Standards – PDF Powder Diffraction File
22. ICSD Collection Code – available on Crystallography Open Database (COD). http://www.crystallography.net